

Phase demodulation with iterative Hilbert transform embeddings

Erik Gengel^a, Arkady Pikovsky^{a,b}

^a*Institute for Physics and Astronomy, University of Potsdam, Karl-Liebknecht Str. 24/25, 14476 Potsdam, Germany*

^b*Department of Control Theory, Institute of Information Technologies, Mathematics and Mechanics, Lobachevsky University Nizhny Novgorod, Russia*

Abstract

We propose an efficient method for demodulation of phase modulated signals via iterated Hilbert transform embeddings. We show that while a usual approach based on one application of the Hilbert transform provides only an approximation to a proper phase, with iterations the accuracy is essentially improved, up to precision limited mainly by discretization effects. We demonstrate that the method is applicable to arbitrarily complex waveforms, and to modulations fast compared to the basic frequency. Furthermore, we develop a perturbative theory applicable to a simple cosine waveform, showing convergence of the technique.

Keywords: Phase modulation, Hilbert transform, Embedding

1. Introduction

Demodulation of nearly oscillatory signals is a standard problem in signal processing. In classical communication schemes, one uses amplitude, phase, and frequency modulations to store information in an analog signal. At the receiving side, demodulation is needed to extract this information. In a more general context, when one tries to characterize the dynamics of an oscillatory system based on some observable, modulation carries important information about the system operation. For example, the electrocardiogram is an important signal characterizing the human cardio-vascular system. One of the widely used tools is demodulation of this signal via extracting information about the instantaneous periods (RR intervals), with further analysis of demodulated heart rate variability [1]. In many situations one considers a demodulation task for harmonic carrying waveforms only (see, e.g., [2]), but in fact one quite often needs to demodulate signals with unknown, potentially rather complex waveform (like the electrocardiogram signal).

In this paper we focus on the problem of demodulation of phase modulated signals with arbitrary waveforms and arbitrary phase modulations. This task is essential for characterization of oscillatory processes resulting from forced and/or coupled self-sustained oscillators, e.g. for synchronization analysis [3–5] and for reconstruction of the phase dynamics [6–8]. In particular, in Refs. [9, 10] a continuous phase was ex-

Email addresses: egengel@uni-potsdam.de (Erik Gengel), pikovsky@uni-potsdam.de (Arkady Pikovsky)

tracted from the electrocardiogram signal, and further used to build a phase model for the cardio-respiratory interaction.

The Hilbert transform (HT) is a widely used tool in oscillatory data analysis and signal processing. It lies at the heart of the analytic signal approach [11–15], which provides an effective processing of nearly harmonic signals. The Hilbert transform is also extensively used for the phase demodulation in synchronization studies [3, 16], see also recent review [17]. One uses it to perform a two-dimensional embedding of the observed signal; this embedding then is usually treated as an analytic signal and the phase is extracted as the argument of the complex state (or, more generally, as an angle of rotation with respect to some point on the embedding plane). This approach gives a good approximation, but not the exact phase demodulation. The quality of the analytic signal based phase demodulation is better for slow modulation, although also in this situation, as will be illustrated below, it is not exact.

One can attribute non-exactness of the HT embedding to the fact, that the HT generally mixes phase and amplitude modulations: if one starts with a purely phase modulated signal, then the HT embedded signal will have amplitude modulation as well. In signal processing, workarounds exist [14, 18] that introduce filtering before application of the HT and/or decomposition of the signal into several functions to avoid the mixing.

In this paper we propose a phase demodulation method based on iterative HT embeddings. The first step is the same as in the traditional approach, it yields an approximation, but the signal is not fully demodulated. We use the phase obtained in the first step as a new time variable to perform the next embedding, with better demodulation. The repetition of this procedure provides better and better approximations. We will demonstrate that the iterations result in a very accurate demodulation with errors related to numerical errors in calculating the Hilbert transform integral. Noteworthy, our method is not restricted to simple waveforms like cosine function; we will present its implementation for arbitrary (but smooth) waveforms. Thus, no filtering is involved in the approach we describe.

For completeness, we mention another class of approaches to phase demodulation, where not the phase itself is determined, but the instantaneous frequency is evaluated via a time-frequency decomposition (see, e.g., [19]). Recently, a variant of this approach – wavelet-based synchrosqueezing – have been suggested [15, 20, 21]. Comparison with these methods is a subject of future research.

The paper is organized as follows. First, in section 2, we elaborate on our definition of the waveform and the phase for a signal, and discuss connections to dynamical systems analysis. Then we present our method in sections 3,4. Analytic results on the convergence of the method, based on a perturbation analysis, are described in section 5. Numerical results, confirming accuracy of the technique for a range of strongly modulated signals and for complex waveforms, are presented in section 6. In section 7, a transformation from a phase variable, obtained in the demodulation procedure, to another phase is discussed. We end with conclusions in section 8.

2. Phase modulated signals

2.1. Definition of a phase modulated signal

The subject of our study are phase-modulated signals. First we define a *waveform* $S(\varphi) = S(\varphi + 2\pi)$ as a 2π -periodic function of its argument. The argument, interpreted as a *phase*, is a monotonous function of time $\dot{\varphi} > 0$. If $\dot{\varphi} \neq \text{const}$, one speaks of a *phase modulated signal*

$$x(t) = S(\varphi(t)) . \quad (1)$$

Our task is, given the signal $x(t)$, to reconstruct the phase $\varphi(t)$ and the waveform $S(\varphi)$.

Our method below is not restricted to simple waveforms: $S(\varphi)$ can be a rather complex function with several maxima and minima. Below in the numerical examples and in theoretical considerations we will use

$$S_1(\varphi) = \cos(\varphi) \quad (2)$$

as a simple waveform, and

$$S_2(\varphi) = \cos(\varphi) - 0.7 \sin(2\varphi) + \cos(3\varphi) \quad (3)$$

as a complex waveform.

2.2. Phase modulation in driven oscillators

The motivation for this setup comes from the inverse problems for nonlinear dynamical systems. Phase modulated signals naturally appear if a dynamical system with stable self-sustained oscillations (i.e. with a limit cycle) is driven by a weak external force (or interacts with another dynamical system) [16, 22–24], as we briefly outline below.

Suppose we have an autonomous dynamical system

$$\dot{\vec{y}} = \vec{F}(\vec{y})$$

with a stable limit cycle $\vec{y}_0(t)$. This means that the system generates periodic oscillations and a generic scalar observable $x(\vec{y})$ is a periodic function of time $x(\vec{y}_0(t))$. On the limit cycle and in its basin of attraction one can introduce the phase variable $\varphi = \Phi(\vec{y})$, such that the limit cycle is parametrized by this phase $\vec{y}_0(\varphi + 2\pi) = \vec{y}_0(\varphi)$, and the phase grows linearly in time with the natural frequency of the limit cycle $\dot{\varphi} = \omega$.

If there is a weak external force acting on the system

$$\dot{\vec{y}} = \vec{F}(\vec{y}) + \varepsilon \vec{P}(\vec{y}, t),$$

then, in the first approximation in ε , a phase-modulated dynamics on the limit cycle represents the full oscillation of $\vec{y}(t)$ close to $\vec{y}_0(\varphi(t))$, where the phase obeys the equation

$$\dot{\varphi} = \omega + \varepsilon Q(\varphi, t) \quad (4)$$

and $Q = \text{grad}\Phi|_{\vec{y}_0(\varphi)} \cdot \vec{P}(\vec{y}_0(\varphi), t)$ is determined by the phase response curve of the limit cycle and the force \vec{P} [25]. Accordingly, the scalar observable x is the phase-modulated signal as described above:

$$x(t) = x(\vec{y}_0(\varphi(t))) .$$

Here the waveform is determined by the form of the limit cycle and of the scalar observable $S(\varphi) = x(\vec{y}_0(\varphi))$. The inverse problem in the context of the theory above is formulated as follows: From scalar observations $x(t)$ of a driven dynamical system, one seeks to reconstruct the dynamics of the phase $\varphi(t)$. The first step here is the reconstruction of the phase $\varphi(t)$, what is the topic of the present study.

2.3. Phase vs protophase

In this section we discuss whether the decomposition of a signal (1) into the phase and the waveform is unique. The answer is obvious: No. Indeed, one can perform a transformation

$$\psi = \Psi(\varphi), \quad \Psi(s + 2\pi) = \Psi(s) + 2\pi, \quad \Psi' > 0, \quad (5)$$

to a new phase variable ψ , in terms of which the signal is represented as

$$x(t) = \tilde{S}(\psi(t)), \quad \tilde{S} = S(\Psi^{-1}(\psi(t)))$$

with the new 2π -periodic waveform $\tilde{S}(\psi) = \tilde{S}(\psi + 2\pi)$. Generally, there is no particular reason to prefer the representation in terms of the waveform S and the phase φ to the representation in terms of the waveform \tilde{S} and of the phase ψ .

In applications, “preferable” phase variables can exist. For example, for a dynamical system where the equation for the phase in form (4) is used, the “true” phase has the property of a uniform (on average) rotation, so that the distribution density of this phase does not depend on the phase itself. See more discussion in Refs. [6], where general possible phase variables have been named “protophases”, and a transformation of form (5) from a protophase to the phase having uniform distribution density has been suggested as a step in the phase reconstruction. However, in other applications other conditions on the phase may be imposed. On the other hand, there can be a “preferable” waveform. For example, a waveform with one maximum and one minimum over the period, can be transformed to a cosine waveform. The ambiguity of the phase definition results also in the ambiguity of the instantaneous frequency, if the latter is defined as the time derivative of the phase.

Summarizing, we state that the decomposition of a signal (1) is not unique, and in different methods, described below, different protophases and correspondingly different waveforms will be obtained. We will, however, consider demodulation as successful, if at least one particular protophase and the corresponding waveform can be found. The success of demodulation means that a protophase $\psi(t)$ is found, such that values of $|x(\psi) - x(\psi + 2\pi)|$ are very small. Quantitatively, we define the squared integrated error of demodulation in Eq. (9) below.

2.4. Link function approach

There is another formulation of the demodulation problem, based on the *link function* approach [M. Holschneider, private communication]. Given a modulated signal (1), one looks for a function of time $L(t)$, called link function, such that

$$x(t + L(t)) = x(t) .$$

If a protophase $\psi(t)$ of the signal is known, then one can define the link function as $\psi(t + L(t)) = \psi(t) + 2\pi$, what can be resolved via the inverse function $t(\psi)$ as $L(t) = t(\psi(t) + 2\pi) - t$. One can easily see that the link function is independent on the choice of the protophase, and in this sense is invariant. For the dynamical systems described in section 2.2, the link function gives the return time for the Poincaré map from the value of the phase to the next value shifted by 2π . The task of finding a protophase if the link function is known, is, to the best of our knowledge, not solved.

3. Proxi-phase extraction

Our main method is based on an iteration procedure. At each iteration stage, an approximation to the phase is extracted from the phase-modulated signal $x(t)$; we call the result of this extraction “proxi-phase” below. In fact, this extraction step is performed only once in most existing approaches to extract the phase dynamics from data (for example, see [6, 10, 26, 27]).

The usual approach is to perform a two-dimensional embedding $x(t) \rightarrow (x(t), y(t))$, so that a phase-modulated signal is represented by “rotations” or “loops” on the plane (x, y) . In the field of dynamical system reconstruction, different choices for y have been discussed, two popular are a delayed signal $y = x(t - \tau)$ and the derivative $y = \frac{dx}{dt}$ [28–30]. However, the mostly stable and reliable results are achieved with the Hilbert transform [3]:

$$y(t) = \hat{H}[x(t)] = \frac{1}{\pi} P.V. \int_{-\infty}^{\infty} \frac{x(t')}{t - t'} dt' . \quad (6)$$

The resulting trajectory on the plane $(x(t), y(t))$ we call HT-embedding.

Below we will consider two basic ways to extract a proxi-phase from the HT embedding. In the simplest case, where the waveform is close to a $\cos(\varphi)$ function, the HT embedding is close to a circle, surrounding the origin (see Fig. 1(a) below), and one can define the proxi-phase $\theta^{(a)}(t)$ as the angle from the origin (or another point close to the origin) to the position of the signal:

$$\theta^{(a)}(t) = \arg[x(t) + iy(t)] . \quad (7)$$

This definition corresponds to the proxi-phase as the argument of the analytic signal $z(t) = x(t) + iy(t)$. Therefore we will call $\theta^{(a)}$ the *analytic proxi-phase*. The proxi-phase $\theta^{(a)}$ should be additionally unwrapped, so that it is a monotonously growing function of time.

This simple definition of the proxi-phase will not work for a complex waveform with several maxima and minima on the period. In this case the embedding on the plane (x, y) has many loops (see Fig. 1(e) below), and the evaluation of the proxi-phase according to (7) is not possible. Even for the simple waveform $S(\varphi) = \cos(\varphi)$, if the phase modulation is strong and the modulation frequency is high, a situation may occur where the analytic proxi-phase according to (7) is non-monotonous. This makes application of the analytic proxi-phase impossible for such cases.

A more universal proxi-phase definition was suggested in Ref. [6] and adopted for the analysis of an electrocardiogram signal in Ref. [9]. This proxi-phase is based on the curve length, to avoid the mentioned problems. The length-based definition of a proxi-phase $\theta^{(b)}(t)$ is

$$\theta^{(b)}(T) = \int_0^T dt \sqrt{\left(\frac{dx}{dt}\right)^2 + \left(\frac{dy}{dt}\right)^2} . \quad (8)$$

For any sufficiently smooth signal, this definition provides a monotonously growing *length proxi-phase*, even if the embedded trajectory has loops.

A small drawback of this definition is that the proxi-phase $\theta^{(b)}(t)$ is not normalized to intervals of 2π at each rotation, contrary to the analytic proxi-phase (7). This does not affect further iteration steps to be described below, because the HT is invariant under rescaling of the function argument. At the very end of the procedure, one can perform the normalization by multiplying $\theta^{(b)}$ with a factor $2\pi\hat{L}^{-1}$, if needed. Here \hat{L} is the average period of the signal in terms of the length (8) after the iteration procedure. To define it, we first define the normalized periodicity error of a function $x(\theta)$, with respect to a period guess L , as

$$\tilde{\varepsilon}(L) = \frac{\int_{\theta_{min}}^{\theta_{max}} (x(\theta' + L) - x(\theta'))^2 d\theta'}{\int_{\theta_{min}}^{\theta_{max}} x^2(\theta') d\theta'} . \quad (9)$$

In case of the analytic proxi-phase, we can set $L = 2\pi$, then expression (9) provides the quality of the phase reconstruction. $\varepsilon = \tilde{\varepsilon}(2\pi)$ only weakly dependent on the protophase definition. If it tends to zero for one protophase, then it tends to zero for other protophases as well.

For the length proxi-phase, the value of L is not known a priori. Here, we obtain an “optimal” period by minimizing the error (9) with respect to L :

$$\hat{L} = \operatorname{argmin}_L \tilde{\varepsilon}(L) , \quad \varepsilon = \min_L \tilde{\varepsilon}(L) = \tilde{\varepsilon}(\hat{L}) .$$

This error will be used in figures 4 and 5 below to quantify quality of demodulation.

The proxi-phase extraction can be viewed as a (nonlinear) operator \hat{P} , providing for a given signal $x(t)$ a proxi-phase

$$\theta(t) = \hat{P}[x(t)]$$

with one of the methods above.

4. Iterated Hilbert transform embeddings

Application of the proxi-phase extraction by one of the methods described in section 3 above shows that this proxi-phase is not the phase, because in the function $x(\theta)$ some phase modulation is still present such that it is not exactly periodic.

We suggest to proceed in an iterative manner: We consider the obtained proxi-phase (which we supply with an index that counts the steps in the iteration process) θ_1 as a new time variable, and apply the proxi-phase extraction to the signal $x(\theta_1)$. Namely, we calculate $\theta_2(\theta_1) = \hat{P}[x(\theta_1)]$, and so on. In other words, we perform iterations

$$\theta_{n+1}(\theta_n) = \hat{P}[x(\theta_n)] \quad (10)$$

The original time can be treated as the zero-index proxi-phase $\theta_0 = t$. To illustrate, we write explicitly the steps for the analytic signal proxi-phase $\theta^{(a)}$:

$$\begin{aligned} y(\theta_n) &= \hat{H}[x(\theta_n)] = \frac{1}{\pi} \text{PV} \int_{-\infty}^{\infty} \frac{x(\theta'_n)}{\theta_n - \theta'_n} d\theta'_n, \\ \theta_{n+1} &= \arg [x(\theta_n) + iy(\theta_n)] . \end{aligned} \quad (11)$$

In numerical implementation of the iterations, one has to perform the HT for a function defined on a non-uniform grid; see Appendix A for the implementation we used.

Our numerical simulations show that this iterative procedure effectively reduces the errors (9), and, with high accuracy, θ_n converges to a correct protophase for large n . Just visually one can check this by comparison of embedded plots $(x(\theta_n), y(\theta_n))$ for different iteration steps n , see Fig. 1. If the signal $x(\theta_n)$ is a periodic function of θ_n , then $y(\theta_n)$ is also a periodic function, and on the embedding plane one observes just a closed curve. Contrary to this, if θ_n is just an approximation and $x(\theta_n)$ is not periodic but contains rest modulation, then one observes a non-closed trajectory forming a sequence of non-equal loops.

In Fig. 1 one can see that just one step in the phase extraction does not provide a good phase – the embeddings in panels (b),(f) look like quite wide bands. In course of iterations, these bands become narrower, and already at the 10-th step one observes very narrow lines (panels (d),(h)), what means that the demodulation procedure is successful.

Below we first present a theory, showing that the proposed iteration method indeed converges for a cosine waveform and a weak modulation. Then, in section 6, we will first check predictions of the theory; and then explore convergence of the method for strong modulations, by virtue of the error analysis according to expression (9).

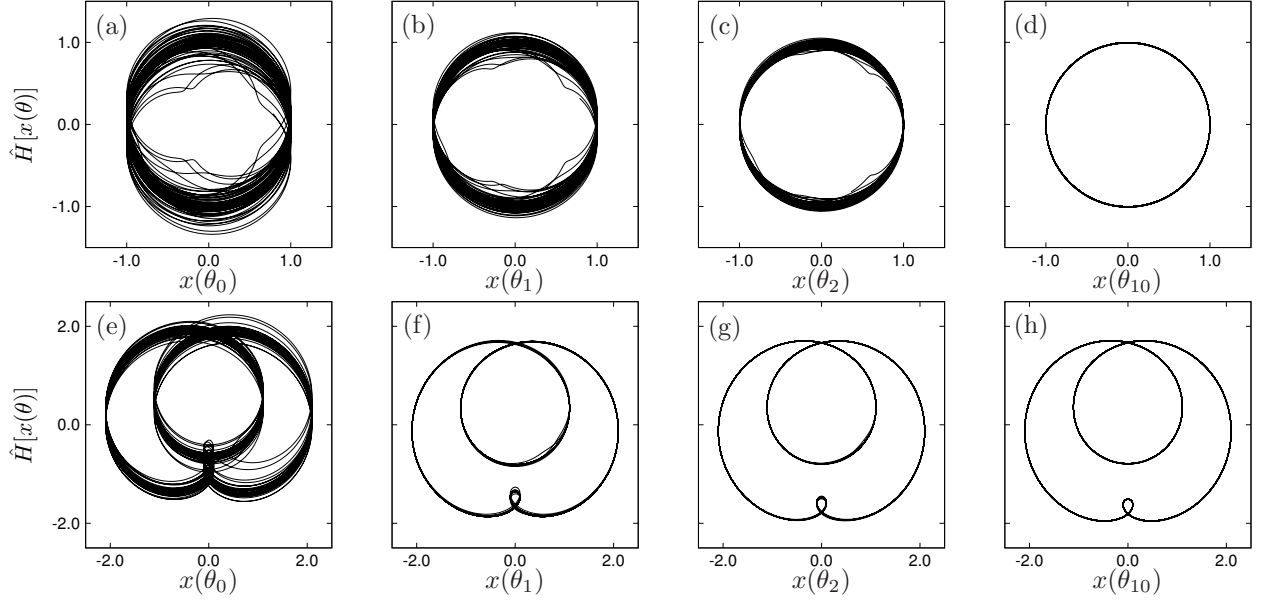


Figure 1: Iterated HT embeddings for the phase-modulated signals $x_{1,2}(t) = S_{1,2}(\varphi(t))$ (see expressions (2,3)) with modulation $\varphi(t) = t + 1.2(\sin(0.25\sqrt{2}t) + \cos(0.25\sqrt{3}t))$. Panels (a)-(d) show the simple waveform case, here the analytic proxi-phase was adopted. Panels (e)-(h) show the complex waveform, here the length proxi-phase was used. The iteration steps: (a),(e): $n = 0$; (b),(f): $n = 1$; (c),(g): $n = 2$, and (d),(h): $n = 10$.

5. Theory

Our strategy here is to show that at each iteration (10) the residue between the true phase and the calculated phase decreases. We represent the modulation of the true phase as

$$\varphi(t) = t + \epsilon q(t), \quad \epsilon \ll 1,$$

and restrict our analysis to terms of first order in ϵ . We have fixed the basic frequency of the signal to one, without loss of generality. Thus, the signal and its HT are represented as

$$\begin{aligned} x(t) &= S(\varphi(t)) \approx S(t) + \epsilon S'(t)q(t), \\ \hat{H}[x](t) &\approx \hat{H}[S(t)] + \epsilon \hat{H}[S'(t)q(t)], \end{aligned} \quad (12)$$

where prime denotes derivative. We calculate both proxi-phases in the first order in ϵ based on (7) and (8) respectively, and obtain general expressions, valid for arbitrary waveforms S and modulations $q(t)$:

$$\begin{aligned} \theta^{(a)}(t) &= \arctan\left(\frac{\hat{H}[S(t)]}{S(t)}\right) + \epsilon \frac{\hat{H}[S'(t)q(t)]S(t) - S'(t)q(t)\hat{H}[S(t)]}{(S(t))^2 + \hat{H}[S(t)]^2} \\ \theta^{(b)}(t) &= \int_0^t \sqrt{(S'(\tau))^2 + \hat{H}[S'(\tau)]^2} d\tau \\ &\quad + \epsilon \int_0^t \frac{S'(\tau)(q'(\tau)S'(\tau) + S''(\tau)q(\tau)) + \hat{H}[S'(\tau)](\hat{H}[q'(\tau)S'(\tau)] + \hat{H}[q(\tau)S''(\tau)])}{\sqrt{(S(\tau))^2 + \hat{H}[S(\tau)]^2}} d\tau \end{aligned} \quad (13)$$

We are able to give compact tractable expressions for the simplest waveform $S(\varphi) = \cos \varphi$ only. This case is treated below.

The difference $\Delta^{(a,b)}(t) = \varphi(t) - \theta^{(a,b)}(t)$ between the true phase and the reconstructed one should be interpreted as the rest modulation after the first iteration. For the analytic proxi-phase (7) and the length based proxi-phase (8), in the case $S(\varphi) = \cos(\varphi)$, the expressions for the rest modulation, obtained through simple calculations from (13), read

$$\Delta^{(a)}(t) = \epsilon \left(q(t) + \cos(t) \hat{H}[q(t) \sin(t)] - q(t) \sin^2(t) \right), \quad (14)$$

$$\Delta^{(b)'}(t) = \frac{\epsilon}{2} q'(t) + \frac{\epsilon}{2} [\cos(2t) q'(t) - \sin(2t) q(t) + 2 \cos(t) \hat{H}[q'(t) \sin(t)] + 2 \cos(t) \hat{H}[q(t) \cos(t)]] . \quad (15)$$

Here, to get rid of the integral in the expression for $\Delta^{(b)}$, we take derivative with respect to time t .

We now use the Bedrosian's theorem [31], which states that the HT of a product of a low-frequency $Q_L(t)$ and a high-frequency $Q_H(t)$ signals and can be represented as

$$\hat{H}[Q_L(t)Q_H(t)] = Q_L(t)\hat{H}[Q_H(t)] .$$

The condition for the Bedrosian's theorem is that the spectra of Q_L and Q_H do not overlap: the whole spectrum of Q_L lies left to the spectrum of Q_H .

Thus, to evaluate the terms $\hat{H}[q(t) \sin(t)]$, $\hat{H}[q(t) \cos(t)]$, and $\hat{H}[q'(t) \sin(t)]$, we represent $q(t)$ as a sum of two components $q(t) = \ell(t) + h(t)$, where the Fourier spectrum of the slow component $\ell(t)$ contains frequencies $|\omega| < 1$, while the Fourier spectrum of the fast component $h(t)$ contains frequencies that obey $|\omega| > 1$. Then, we obtain

$$\hat{H}[q(t) \sin t] = \hat{H}[(\ell(t) + h(t)) \sin(t)] = -\ell(t) \cos(t) + \hat{H}[h(t)] \sin(t) ,$$

and similar for $\hat{H}[q(t) \cos(t)]$ and $\hat{H}[q'(t) \sin(t)]$. Substituting this in (14),(15), we see that the component $\ell(t)$ does not contribute to the rest modulation. Only the contribution of the high-frequency component remains:

$$\Delta^{(a)}(t) = \frac{\epsilon}{2} h(t) + \frac{\epsilon}{2} \left(h(t) \cos(2t) + \sin(2t) \hat{H}[h(t)] \right), \quad (16)$$

$$\Delta^{(b)'}(t) = \frac{\epsilon}{2} h'(t) + \frac{\epsilon}{2} \left(\hat{H}[h(t)] + \cos(2t) h'(t) - \sin(2t) h(t) + \sin(2t) \hat{H}[h'(t)] + \cos(2t) \hat{H}[h(t)] \right) . \quad (17)$$

At this stage, it is more convenient to operate with the Fourier spectra $\mathcal{F}_h(\omega), \mathcal{F}_\Delta(\omega)$ of functions $\epsilon h(t), \Delta(t)$. The Hilbert transform in the Fourier space has the form $\mathcal{F}(\hat{H}[h(t)])(\omega) = -i \operatorname{sgn}(\omega) \mathcal{F}_h(\omega)$. Application of the Fourier transform to expressions (16) and (17) yields:

$$\begin{aligned} \mathcal{F}_{\Delta^{(a)}}(\omega) &= \frac{1}{2} \left[\mathcal{F}_h(\omega) + \frac{1}{2}(1 - \operatorname{sgn}(\omega - 2))\mathcal{F}_h(\omega - 2) + \frac{1}{2}(1 + \operatorname{sgn}(\omega + 2))\mathcal{F}_h(\omega + 2) \right], \\ \mathcal{F}_{\Delta^{(b)'}}(\omega) &= \frac{1}{2} \left[\frac{\omega - \operatorname{sgn}(\omega)}{\omega} \mathcal{F}_h(\omega) + \left(\frac{\omega - 1}{\omega} (1 - \operatorname{sgn}(\omega - 2))\mathcal{F}_h(\omega - 2) + \right. \right. \\ &\quad \left. \left. \frac{\omega + 1}{\omega} (1 + \operatorname{sgn}(\omega + 2))\mathcal{F}_h(\omega + 2) \right) \right]. \end{aligned} \quad (18)$$

We now use that $\mathcal{F}_h(\omega) = 0$ for $|\omega| < 1$, what allows us to simplify expressions (18) to

$$\mathcal{F}_\Delta(\omega) = \begin{cases} A(\omega)\mathcal{F}_h(\omega) + B(\omega)\mathcal{F}_h(\omega + 2) & \text{if } \omega > 1, \\ B(\omega)\mathcal{F}_h(\omega + 2) + A(\omega)\mathcal{F}_h(\omega - 2) & \text{if } -1 < \omega < 1, \\ B(\omega)\mathcal{F}_h(\omega) + A(\omega)\mathcal{F}_h(\omega - 2) & \text{if } \omega < -1, \end{cases} \quad (19)$$

where

$$A(\omega) = B(\omega) = 1/2 \text{ for the analytic proxi-phase } \Delta^{(a)}, \quad (20)$$

$$A(\omega) = \frac{\omega \mp 1}{2\omega}, \quad B(\omega) = \frac{\omega \pm 1}{2\omega} \text{ for the length proxi-phase } \Delta^{(b)}.$$

In (20), the upper sign is used for $\omega > 1$ and the lower sign is used for $\omega < -1$.

Relation (19) can be considered as a transformation of the rest phase modulation at a step of our iteration procedure. Denoting the spectrum of the high-frequency modulation $\epsilon h(t)$ at the n -th step of the iteration procedure as \mathcal{F}_n , we can write a general recursion formula for the evolution of this spectrum under iterations:

$$\mathcal{F}_{n+1}(\omega) = \begin{cases} A(\omega)\mathcal{F}_n(\omega) + B(\omega)\mathcal{F}_n(\omega + 2) & \text{if } \omega > 1, \\ B(\omega)\mathcal{F}_n(\omega + 2) + A(\omega)\mathcal{F}_n(\omega - 2) & \text{if } -1 < \omega < 1, \\ B(\omega)\mathcal{F}_n(\omega) + A(\omega)\mathcal{F}_n(\omega - 2) & \text{if } \omega < -1. \end{cases} \quad (21)$$

This relation is the main result of our weak modulation analysis. We now discuss its meaning for the iteration procedure of demodulation (where we focus, due to the evident symmetry, on positive frequencies only).

1. The first observation is that in both cases of proxi-phase definition, slow modulation (i.e. with frequencies lower than the basic oscillation frequency) is resolved exactly already in the first iteration. This is a well-known empirical fact that the traditional HT phase extraction (where only the first iteration is used) works well for slow modulation, but is not so good for fast modulation.
2. The high-frequency components do not disappear immediately, but are, on one hand, damped by factor $A(\omega)$, and on the other hand, produce components shifted to lower frequencies and damped by factor $B(\omega)$. Schematically, this is illustrated in Fig. 2. This scheme shows that for all spectra decaying at infinity, i.e. with $\lim_{\omega \rightarrow \infty} |\mathcal{F}_0(\omega)| = 0$, the modulation eventually disappears, i.e. $\lim_{n \rightarrow \infty} |\mathcal{F}_n(\omega)| = 0$. For some important classes of spectra, one can show that the eigenvalues of the transformation operator (21) are smaller than one (see Appendix B), so that the iteration procedure converges exponentially. In particular, for spectra $\mathcal{F}_h(\omega)$ which decay exponentially $\mathcal{F}_h(\omega) \sim \exp[-\alpha\omega]$ (what corresponds to a smooth modulation $h(t)$), we have $|\mathcal{F}_n| \sim (1 + \exp[-2\alpha]/2)^n \xrightarrow{n \rightarrow \infty} 0$.
3. In the analysis above we have not considered components of modulation having frequencies 1, 3, 5, ..., i.e. harmonics of the basic oscillation frequency. Such components cannot be demodulated, because one cannot distinguish them from the original phase – in fact, a modulation with these frequencies is equivalent to changing the shape of the waveform $S(\varphi)$.

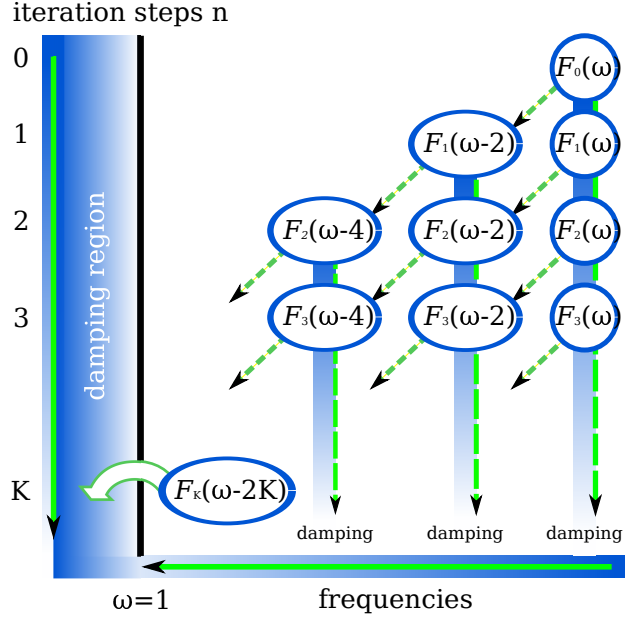


Figure 2: Depicted is the damping of Fourier modes in the range $2K < \omega < 2K + 2$ for the simple waveform $S(\varphi) = \cos(\varphi)$. In each iteration step, the method damps $\mathcal{F}_n(\omega)$ (dashed vertical arrows) and additionally generates a new Fourier mode at a smaller frequency (dashed diagonal arrows). At step K , a Fourier mode with frequency less than 1 is generated in the low-frequency region (bold green-white arrow), where it disappears before the next iteration. The damping factors are given by (20).

6. Numerical tests

6.1. Testing theoretical relations

Our first numerical example is intended to illustrate the theory of Section 5. Therefore, we use here the simple waveform $S(\varphi) = \cos(\varphi)$, and the modulation is a function of time

$$\varphi(t) = t + a \sin(ft) + b \cos(gt), \quad (22)$$

possessing two frequencies f and g . We performed iterative HT embeddings as described above, calculated at each step the analytic proxi-phase, and found the spectral components of the differences $\theta_n^{(a)}(t) - \varphi(t)$. These spectral components are presented in Fig. 3 for four numerical setups.

Case (a). Panel (a) of Fig. 3 shows the case $a = 0$, $b = 0.2$, $g = 3.73$ of a single-harmonic modulation with high frequency. Here the modulation is relatively weak, and we expect relations (19) to hold. One can indeed see that, in agreement with the theory, $\theta_1^{(a)} - \varphi$ contains harmonics at frequencies g and $g - 2$ with the same amplitude. At the next iteration, the component at g decreases by factor 2, while the component at $g - 2$ remains the same; additionally a component with frequency $|g - 4|$ appears. Also at iterations 3 and 4, relation (21) is well fulfilled.

Case (b). Panel (b) illustrates nonlinear effects at a strong low-frequency single-harmonic modulation. Here $a = 1$, $f = 0.41$, and $b = 0$. One can see that although the frequency of modulation is less than

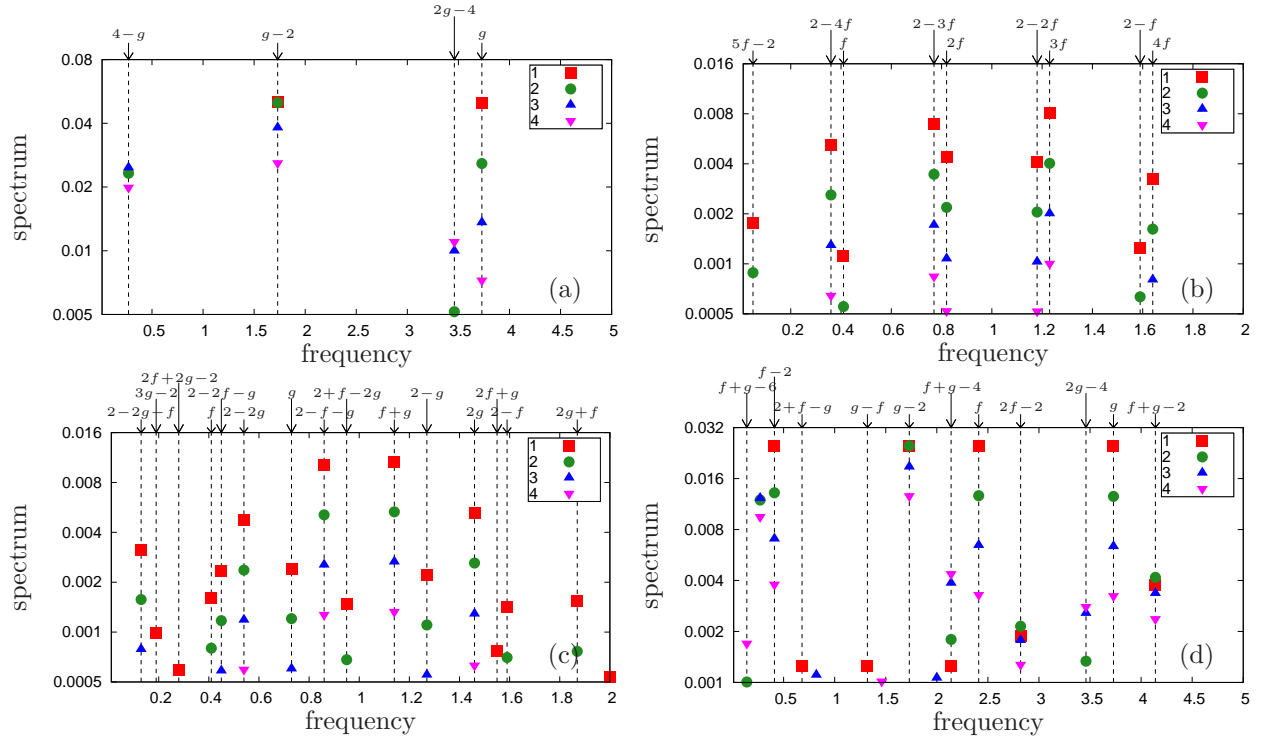


Figure 3: We show the most essential spectral components of the phase demodulation error $\theta_n^{(a)} - \varphi$ for the first 4 iterations (squares, circles, up and bottom triangles, respectively). The observed spectral components are marked with arrows on top of panels. In all cases the original signal is $x(t) = \cos(\varphi(t))$, where the modulation is given by Eq. (22). The vertical scale is logarithmic, with the ticks marking factor 2, to allow for a visual comparison with the theory, where the damping factors are $1/2$.

one, this component at f does not disappear completely in $\theta_1^{(a)} - \varphi$ as predicted by the linear theory, but is finite (already rather small). In the first iteration higher harmonics nf and the combinational frequencies $nf - 2$ appear, and they are relatively large. During next iterations the amplitudes of these components decrease with a factor $\approx 1/2$.

Case (c). Panel (c) shows the case of relatively strong two-frequency modulation, where both frequencies are low: $a = b = 0.3$, $f = 0.41$, $g = 0.73$. Due to nonlinearity, many combinational frequencies $kf + lg$, $kl + fg - 2$ with integers k and l are excited. It appears that all the new frequencies, like in case (b), are created in the first iteration, further iterations follow roughly the law (21).

Case (d). Panel (d) shows, like case (c), a strong two-frequency modulation, but with high basic frequencies $a = b = 0.1$, $f = 2.41$, $g = 3.73$. One can see that at some combinational frequencies, the level even initially increases due to the cascade process of amplitude shifting (see, e.g., components with $f + g - 4$), and one needs more iterations to reduce error at these components.

In conclusion, the presented numerical tests show that the theory based on the linear approximation works well for weak modulation, but for strong modulation, there are essential nonlinear effects at the first few iterations. Because the effective modulations become weaker in the course of iterations, the theory better describes higher iterations.

6.2. Accuracy of the iterative procedure

In the following, we present numerical results for the signals $x(t) = S_{1,2}(\varphi(t))$, where the waveforms are given by expressions (2),(3), and the phase modulation is a quasiperiodic function of time

$$\varphi(t) = t + \frac{a}{R} \cos(R\omega_1 t) + \frac{b}{R} \cos(R\omega_2 t) . \quad (23)$$

We have chosen $\omega_1 = \sqrt{2}$, $\omega_2 = \sqrt{3}$, $a = b = 0.3$. Parameter R allows us to vary the basic frequencies, keeping the range of the phase modulation (which is quite large, $\min(\dot{\varphi}) = 1 - a(\omega_1 + \omega_2) \approx 0.056$, so the first-order theoretical analysis of section 5 is not applicable) constant. In all runs we used discretisation step $\Delta t = 0.002$, the length of the time series was about 95 basic periods. Convergence was characterized by evaluating error (9), where, to discard boundar effects, only central 80% of the time series were used.

Our goal is to quantify performance of the iterative procedure described, in dependence on the characteristic time scale defined by parameter R , on the properties of the waveform (simple vs complex), and on the choice of proxi-phase in the iterative process (analytic vs length-based).

6.2.1. Simple waveform: comparison of analytic and length-based proxi-phases

For the simple waveform (2), one can use both proxi-phases - the analytic one and the length-based one. The results are shown in Fig. 4. One can see that both proxi-phases ensure demodulation with a very small

rest error, if the modulation is slow ($R \leq 1$). For the lowest-frequency case, the length method performs even significantly better at high iterations.

For larger values of $R \geq 2$, the length method appears to be the only applicable one. Here, the analytic proxi-phase fails because at one of the first iterations the analytic proxi-phase becomes a non-monotonous function of time, and iterations break. In contradistinction, the length-based phase always provides a monotonous estimate of the phase. One can see that for the fastest modulation explored ($R = 8$), the error decreases not monotonously with n (it increases at $n \gtrsim 10$), but even in this case, the error of the iteration procedure eventually becomes rather small.

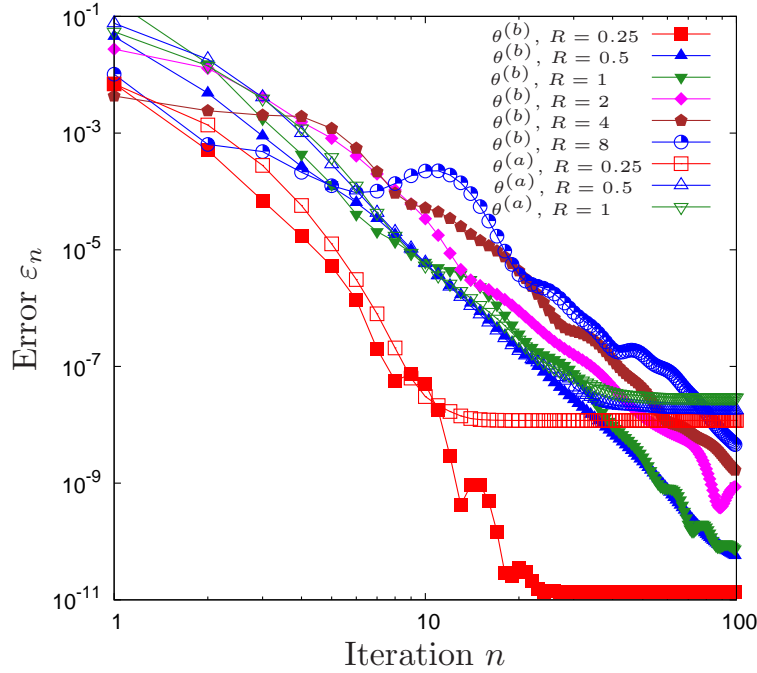


Figure 4: Errors of demodulation for simple waveform S_1 and both proxi-phases calculations in dependence on the iteration index n and R . For $R = 0.25, 0.5, 1$, results for the analytic and length proxiphases are depicted in the same color, but with open and filled markers, respectively.

6.2.2. Complex waveform

For the complex waveform (3), only the length-based phase can be used. In Fig. 5 we show the errors vs the iteration number n , for the same values of the parameter R as in Fig. 4. In all cases the final error is very small, close to $10^{-7} - 10^{-8}$. Similarly to the case of the simple waveform, here at the fastest example ($R = 8$), the demodulation is not monotonous.

The presented results confirm that the described method provides an effective demodulation of the complex signal. We attribute the rest error to numerical inaccuracies in calculation of the HT, of the length of the trajectory on the plane (x, y) , and in the evaluation of the error itself. This is supported by the observation that the asymptotic errors grow significantly if a larger discretization step is used.

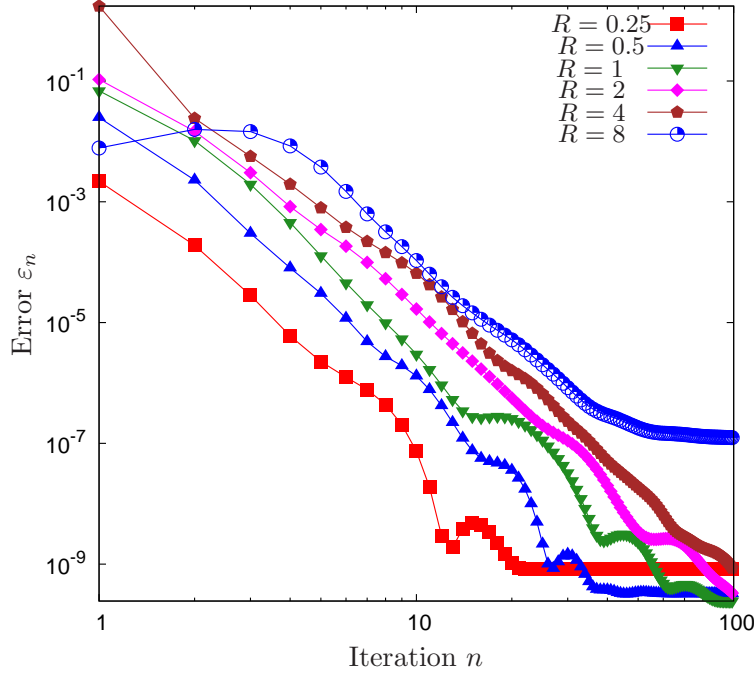


Figure 5: Errors of demodulation in dependence on the iteration index n and R for the complex waveform S_2 .

It is important to mention, that contrary to the analytic proxi-phase (7) which is 2π -periodic, the length-based proxi-phase (8) does not have a “natural” period: strictly speaking, a proper normalization to period 2π is only possible at the end stage of the iteration procedure, where the periodicity of $x(\theta^{(b)})$ is well-defined.

6.3. Arbitrary phase modulation

Above we considered phase modulations as quasiperiodic deviations from the linear phase growth. The method is, however, not restricted to such cases. As an example, we present here results for the complex waveform S_2 (Eq. (3)) with phase modulation defined as $\dot{\varphi} = \Omega(t)$, with a rather arbitrarily chosen instantaneous frequency

$$\Omega(t) = -2\tau + 0.5 \exp(2\tau) + \exp[-100(\tau)^2] + 0.2 \cos(\sqrt{2600}\tau), \quad \tau = \frac{t}{200\pi}, \quad -200\pi \leq t < 200\pi, \quad (24)$$

see Fig. 6(b). For the sampling with $\Delta t = 0.005$, the demodulation error $\approx 3 \cdot 10^{-8}$ was achieved after 20 iterations (see Fig. 6(c)). In Fig. 6(a) the quality of demodulation is illustrated visually, like in Fig. 1.

7. Transformation of a protophase to true phase

As discussed in section 2.3 above, there is an intrinsic ambiguity in the phase demodulation problem: one can perform a transformation of a waveform together with a transformation of an obtained protophase, such that the signal remains the same. Thus, one needs additional conditions to specify a particular phase and a particular waveform uniquely. In the context of the dynamical system applications (section 2.2), a

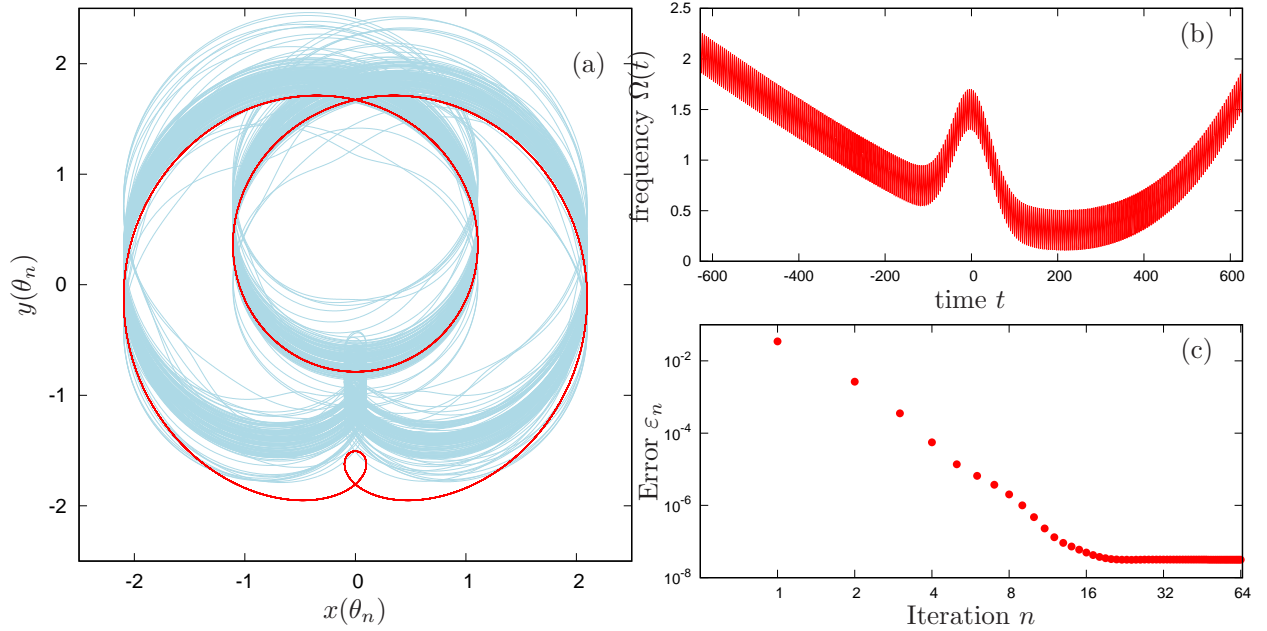


Figure 6: Demodulation of a signal having complex waveform S_2 and the instantaneous frequency (24) (panel (b)). Panel (a) shows embeddings for the original signal $x(\theta_0)$ (blue line) and for the iteration $x(\theta_{64})$ (red line). Panel (c): Errors in dependence on the iteration number.

natural condition is that the phase should grow on average uniformly in time. This condition was adopted in [6], where a procedure for the transformation $\theta \rightarrow C(\theta)$ from a protophase to the uniformly on average growing phase was described. Roughly speaking, for a wrapped protophase one determines the probability distribution density on the interval $[0, 2\pi)$, and performs a transformation such that the new phase has the uniform distribution density. To illustrate this approach, we take an example from section 6.2.2 with $x(t) = S_2(\varphi(t))$, where S_2 is given by Eq. (3) and $\varphi(t)$ is given by Eq. (22) with $R = 8$. In Fig. 7 we show the protophase obtained via the length proxi-phase method, and its transformation according to method [6]. The transformed phase is close to the original one, up to an unavoidable, but unimportant, shift. We stress here, that the accuracy of the transformation $\theta \rightarrow C(\theta)$ is rather weak, because it relies on the empirical probability density, which one obtains based on finite-size data.

8. Conclusion

In summary, we have proposed a method of phase demodulation based on the iterative HT embeddings. In all tested cases it leads to an effective accurate reconstruction of the waveform and of the phase of the signal, up to unavoidable ambiguity due to protophase variety. Our method can be applied to simple and complex waveforms. In all cases we have found that the proxi-phase extraction based on the length of the embedded trajectory is superior to a traditional definition based on the analytic signal.

We have performed theoretical analysis valid for a weak modulation of the simplest cosine waveform.

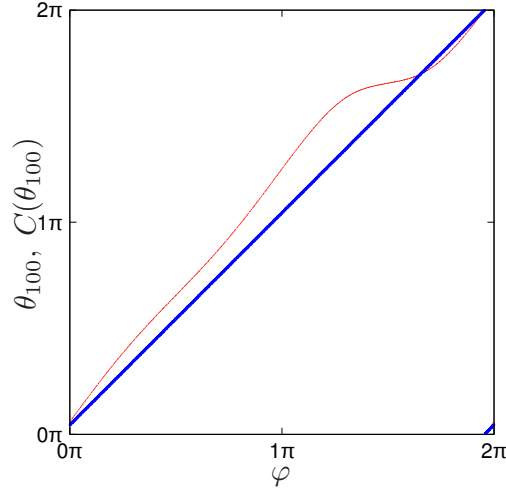


Figure 7: Red points: values of the reconstructed protophase $\theta_{100}^{(b)}$ at 100-th iteration vs. the true phase φ . Blue bold points: the transformed protophase $C(\theta_{100})$. One can see that the relation between $C(\theta_{100})$ and φ is nearly linear.

This analysis shows that while slow modulation is detected exactly already within the first iteration, for fast components the iterations are indeed needed. Furthermore, this analysis yields exponential (in number of iterations) convergence rate for modulation signals which spectra decay exponentially at high frequencies. We have shown also that nonlinear effects in the case of not so weak modulation lead to appearance of combinational frequencies in the modulation spectrum, what nevertheless does not prevent eventual convergence of the procedure.

In this study we considered only regular signals and used a quite high sampling rate. This is mainly to achieve the highest possible performance, because larger discretization steps lead to errors in calculations of the Hilbert transforms. The analysis of different factors affecting the accuracy will be subject of further research. Also applications of the method to practical situations of signals from forced dynamical systems are now under consideration and will be reported elsewhere.

Acknowledgement

A. P. was supported by Russian Science Foundation (Grant No. 17-12-01534). E. G. was supported by Friedrich-Ebert Stiftung. We thank Michael Rosenblum, Michael Feldman, and Mathias Holschneider for their advices and fruitful discussions.

Bibliography

References

- [1] G. Billman, Heart rate variability – a historical perspective, *Front Physiol.* 2 (2011) 86.
- [2] M. P. Fitz, *Fundamentals of Communication Systems*, McGraw-Hill, New York, 2007.
- [3] M. Rosenblum, A. Pikovsky, J. Kurths, C. Schäfer, P. A. Tass, Phase synchronization: from theory to data analysis, in: *Handbook of biological physics*, Vol. 4, Elsevier, 2001, pp. 279–321.

- [4] M. Le Van Quyen, J. Foucher, J.-P. Lachaux, E. Rodríguez, A. Lutz, J. Martinerie, F. J. Varela, Comparison of hilbert transform and wavelet methods for the analysis of neuronal synchrony, *Journal of Neuroscience Methods* 111 (2) (2001) 83–98.
- [5] R. Quiñan Quiroga, A. Kraskov, T. Kreuz, P. Grassberger, Performance of different synchronization measures in real data: A case study on electroencephalographic signals, *Phys. Rev. E* 65 (2002) 041903.
- [6] B. Kralemann, L. Cimponeriu, M. Rosenblum, A. Pikovsky, R. Mrowka, Phase dynamics of coupled oscillators reconstructed from data, *Physical Review E* 77 (6) (2008) 066205.
- [7] L. Q. English, Z. Zeng, D. Mertens, Experimental study of synchronization of coupled electrical self-oscillators and comparison to the sakaguchi-kuramoto model, *Phys. Rev. E* 92 (2015) 052912.
- [8] T. Stankovski, T. Pereira, P. V. E. McClintock, A. Stefanovska, Coupling functions: Universal insights into dynamical interaction mechanisms, *Rev. Mod. Phys.* 89 (2017) 045001.
- [9] B. Kralemann, M. Frühwirth, A. Pikovsky, M. Rosenblum, T. Kenner, J. Schaefer, M. Moser, *In vivo* cardiac phase response curve elucidates human respiratory heart rate variability, *Nature Communications* 4 (2013) 2418.
- [10] Ç. Topçu, M. Frühwirth, M. Moser, M. Rosenblum, A. Pikovsky, Disentangling respiratory sinus arrhythmia in heart rate variability records, *Physiological Measurement* 39 (5) (2018) 054002.
- [11] D. Gabor, Theory of communication. part I: The analysis of information, *Journal of the Institution of Electrical Engineers-Part III: Radio and Communication Engineering* 93 (26) (1946) 429–441.
- [12] E. Bedrosian, The analytic signal representation of modulated waveforms, *Proceedings of the IRE* 50 (10) (1962) 2071–2076.
- [13] D. Vakman, On the analytic signal, the Teager-Kaiser energy algorithm, and other methods for defining amplitude and frequency, *IEEE Trans. Sign. Process.* 44 (1996) 791–797.
- [14] M. Feldman, Hilbert transform applications in mechanical vibration, John Wiley & Sons, 2011.
- [15] D. Iatsenko, P. V. McClintock, A. Stefanovska, Linear and synchrosqueezed timefrequency representations revisited: Overview, standards of use, resolution, reconstruction, concentration, and algorithms, *Digital Signal Processing* 42 (2015) 1–26.
- [16] A. Pikovsky, M. Rosenblum, J. Kurths, Synchronization: a universal concept in nonlinear sciences, Cambridge University Press, 2001.
- [17] J. Sun, Z. Li, S. Tong, Inferring functional neural connectivity with phase synchronization analysis: A review of methodology, *Computational and Mathematical Methods in Medicine* 2012 (2012) 239210.
- [18] P. Kuklik, S. Zeemering, B. Maesen, J. Maessen, H. J. Crijns, S. Verheule, A. N. Ganesan, U. Schotten, Reconstruction of instantaneous phase of unipolar atrial contact electrogram using a concept of sinusoidal recomposition and Hilbert transform, *IEEE transactions on Biomedical Engineering* 62 (1) (2015) 296–302.
- [19] S. Aviñente, A. Y. Mutlu, A time-frequency-based approach to phase and phase synchrony estimation, *IEEE Trans. Sign. Process.* 59 (2011) 3086–3098.
- [20] I. Daubechies, J. Lu, H.-T. Wu, Synchrosqueezed wavelet transforms: An empirical mode decomposition-like tool, *Appl. Comput. Harmon. Anal.* 30 (2011) 243–261.
- [21] D. Iatsenko, P. McClintock, A. Stefanovska, Extraction of instantaneous frequencies from ridges in timefrequency representations of signals, *Signal Processing* 125 (2016) 290 – 303.
- [22] A. T. Winfree, *The Geometry of Biological Time*, Springer, Berlin, 1980.
- [23] Y. Kuramoto, *Chemical Oscillations, Waves and Turbulence*, Springer, Berlin, 1984.
- [24] G. B. Ermentrout, D. H. Terman, *Mathematical foundations of neuroscience*, Vol. 35 of *Interdisciplinary Applied Mathematics*, Springer, New York, 2010.
- [25] E. Brown, J. Moehlis, P. Holmes, On the phase reduction and response dynamics of neural oscillator populations, *Neural Computation* 16 (4) (2004) 673–715.
- [26] D. Benitez, P. Gaydecki, A. Zaidi, A. Fitzpatrick, The use of the Hilbert transform in ECG signal analysis, *Computers in Biology and Medicine* 31 (5) (2001) 399–406.
- [27] K. A. Blaha, A. Pikovsky, M. Rosenblum, M. T. Clark, C. G. Rusin, J. L. Hudson, Reconstruction of two-dimensional phase dynamics from experiments on coupled oscillators, *Physical Review E* 84 (4) (2011) 046201.
- [28] H. Kantz, T. Schreiber, *Nonlinear Time Series Analysis*, Cambridge University Press, Cambridge, 2004, 2nd edition.
- [29] H. Kim, R. Eykholt, J. Salas, Nonlinear dynamics, delay times, and embedding windows, *Physica D: Nonlinear Phenomena* 127 (1-2) (1999) 48–60.
- [30] C. Letellier, J. Maquet, L. Le Sceller, G. Gouesbet, L. Aguirre, On the non-equivalence of observables in phase-space reconstructions from recorded time series, *Journal of Physics A: Mathematical and General* 31 (39) (1998) 7913.
- [31] E. Bedrosian, A product theorem for Hilbert transforms, *Proceedings of the IEEE* 51 (5) (1963) 868–869.
- [32] C. Zhou, L. Yang, Y. Liu, Z. Yang, A novel method for computing the Hilbert transform with Haar multiresolution approximation, *J. Comp. Appl. Math.* 223 (2009) 585–597.

Appendix A. Numerical implementation of the Hilbert transform on a non-uniform grid

The HT of a function $u(\phi)$ is defined as

$$H(\psi) = \frac{1}{\pi} \text{PV} \int_{-\infty}^{\infty} \frac{u(\phi)}{\psi - \phi} d\phi.$$

Suppose the function u is given on a discrete set of points $\phi_1, \phi_2, \dots, \phi_N$ as values u_1, u_2, \dots . We now want to find H_i in the same set of points $\psi_1 = \phi_1, \dots$.

We apply the trapezoidal rule, similar to the approach of [32] for a uniform grid, and write the integral as a sum of elementary integrals over domains (ϕ_k, ϕ_{k+1}) :

$$H(\phi_i) = \frac{1}{\pi} \sum_{k=1}^{N-1} \int_{\phi_k}^{\phi_{k+1}} \frac{u(x)}{\phi_i - x} dx = \frac{1}{\pi} \sum_{k=1}^{N-1} I_k .$$

We approximate $u(x)$ on the interval (ϕ_k, ϕ_{k+1}) by a linear function:

$$u(x) = u_k + \frac{(u_{k+1} - u_k)}{\phi_{k+1} - \phi_k} (x - \phi_k) = a_k + b_k x ,$$

where

$$a_k = \frac{u_k \phi_{k+1} - u_{k+1} \phi_k}{\phi_{k+1} - \phi_k} , \quad b_k = \frac{u_{k+1} - u_k}{\phi_{k+1} - \phi_k} .$$

Thus, the elementary integrals are

$$I_k = \int_{\phi_k}^{\phi_{k+1}} \frac{a_k + b_k x}{\phi_i - x} dx = u_k - u_{k+1} - \frac{u_k \phi_{k+1} - u_{k+1} \phi_k + \phi_i (u_{k+1} - u_k)}{\phi_{k+1} - \phi_k} \ln \left| \frac{\phi_{k+1} - \phi_i}{\phi_k - \phi_i} \right| .$$

This expression is valid for $k \neq i, k \neq i-1$.

To calculate the integrals around ϕ_i , we represent $u = u_i + d_+(x - \phi_i)$ on $\phi_i < x < \phi_{i+1}$ and $u = u_i + d_-(x - \phi_i)$ on $\phi_{i-1} < x < \phi_i$, where

$$d_+ = \frac{u_{i+1} - u_i}{\phi_{i+1} - \phi_i}, \quad d_- = \frac{u_i - u_{i-1}}{\phi_i - \phi_{i-1}} .$$

Then

$$\begin{aligned} I_{i-1} + I_i &= \int_{\phi_{i-1}}^{\phi_{i+1}} \frac{u_i}{\phi_i - x} dx - d_+(\phi_{i+1} - \phi_i) - d_-(\phi_i - \phi_{i-1}) = \\ &= u_i \ln \frac{\phi_i - \phi_{i-1}}{\phi_{i+1} - \phi_i} - d_+(\phi_{i+1} - \phi_i) - d_-(\phi_i - \phi_{i-1}) = u_i \ln \frac{\phi_i - \phi_{i-1}}{\phi_{i+1} - \phi_i} - u_{i+1} + u_{i-1} . \end{aligned}$$

Appendix B. Eigenvalues and eigenfunctions of the modulation iteration operator

Here we explore properties of the transformation operator, acting on the Fourier spectrum of the modulation according to (21)

$$\hat{T}F(\omega) = A(\omega)F(\omega) + B(\omega)F(\omega + 2) , \quad \omega > 1 .$$

Here we restrict our attention to the case $\omega > 1$ only, because negative frequencies are symmetric to positive ones. The real factors $A, B > 0$ are given by (20).

First, we employ the triangle inequality

$$\|A(\omega)F(\omega) + B(\omega)F(\omega + 2)\| \leq A(\omega)\|F(\omega)\| + B(\omega)\|F(\omega + 2)\| ,$$

and restrict our attention to real positive functions $F(\omega)$ only. We look for eigenfunctions of the operator \hat{T} in the class of exponentially decreasing functions of ω at large frequencies: $F(\omega) \sim \exp[-\alpha\omega]$. This means that we consider smooth modulations only. With an ansatz

$$F(\omega) = f(\omega) \exp[-\alpha\omega] ,$$

where $f(\omega)$ has finite variation at $\omega \rightarrow \infty$, the problem reduces to finding eigenfunctions and eigenvalues of the operator

$$\hat{T}_\alpha f(\omega) = A(\omega)f(\omega) + B(\omega)e^{-2\alpha}f(\omega+2) . \quad (\text{B.1})$$

In the simplest case of the analytic proxi-phase, where $A = B = \frac{1}{2}$, one can see that any periodic function $f(\omega) = f(\omega+2)$ is an eigenfunction of (B.1) with eigenvalue

$$\lambda(\alpha) = [1 + \exp(-2\alpha)]/2 < 1 . \quad (\text{B.2})$$

This shows that under action of the operator \hat{T} , the spectral function tends to zero exponentially, the exponent depends on the asymptotics of the spectrum at large frequencies.

In the case of the length proxi-phase, where $A(\omega) = \frac{\omega-1}{2\omega}$ and $B(\omega) = \frac{\omega+1}{2\omega}$, we cannot find the eigenfunctions, but can show that the eigenvalues are the same as for the case $A = B = 1/2$. Indeed, the eigenvalue problem $\hat{T}_\alpha f = \lambda_\alpha f$ reduces, after substitution to (B.1), to a recursion

$$f(\omega+2) = \frac{\lambda_\alpha - A(\omega)}{B(\omega)e^{-2\alpha}} f(\omega) .$$

Because asymptotically $f(\omega)$ should neither grow nor decay at $\omega \rightarrow \infty$, we have

$$\lim_{\omega \rightarrow \infty} \frac{\lambda_\alpha - A(\omega)}{B(\omega)e^{-2\alpha}} = \frac{\lambda_\alpha - \frac{1}{2}}{\frac{1}{2}e^{-2\alpha}} = 1 .$$

This yields the same eigenvalue (B.2).